

## Carrier capture dynamics of InAs/GaAs quantum dots

T. Piwonski,<sup>a)</sup> I. O'Driscoll, J. Houlihan,<sup>b)</sup> G. Huyet,<sup>c)</sup> and R. J. Manning  
 Tyndall National Institute, Lee Maltings, Prospect Row, Cork, Ireland

A. V. Uskov  
 P.N. Lebedev Physical Institute, Moscow, Russia 119991 GSP-1

(Received 27 January 2007; accepted 16 February 2007; published online 20 March 2007)

Carrier dynamics of a 1.3  $\mu\text{m}$  InAs/GaAs quantum dot amplifier is studied using heterodyne pump-probe spectroscopy. Measurements of the recovery times versus injection current reveal a power law behavior predicted by a quantum dot rate equation model. These results indicate that Auger processes dominate the carrier dynamics. © 2007 American Institute of Physics.

[DOI: 10.1063/1.2715115]

Quantum dot (QD) photonic materials have attracted much study in recent years as they have the potential to deliver the stability and coherence of atomic sources within a compact and efficient semiconductor device.<sup>1</sup> Characteristics such as reduced sensitivity to optical feedback and reduced alpha parameter have made such materials attractive as laser sources.<sup>2</sup> Also, the suppression of pattern effects in QD semiconductor optical amplifiers (SOAs) shows promise for high speed applications.<sup>3,4</sup> The understanding of the high speed carrier dynamics of these materials is crucial for their optimization and exploitation. To address this issue, time-resolved spectroscopy has been used to investigate the fundamental carrier decay time scales of SOA structures and determine their suitability for high speed applications. Such pump-probe studies are usually performed using pulse widths of a few hundred femtoseconds to picoseconds in order to sufficiently resolve the relaxation dynamics of high speed devices.<sup>5</sup>

In this letter, we apply such techniques to the study of InAs/GaAs QD SOAs emitting near 1.3  $\mu\text{m}$ . Similar QD devices have been studied previously and, in general, it was shown that the carrier dynamics in QDs can be described by three characteristic time scales; an initial ultrafast component with a time scale of 100s of femtoseconds to picoseconds and commonly related to intradot scattering,<sup>6–8</sup> an intermediate component of up to 10s of picosecond duration,<sup>7,8</sup> commonly attributed to the capture of carriers into the dot and a much longer time (100s of picoseconds) related to the refilling of carriers into the wetting layer.<sup>4,9</sup> In addition, several authors have already pointed out the role of Auger effects in the carrier dynamics of quantum dot devices. For example, previous studies of the threshold current density of lasers as a function of temperature have shown that carrier interband relaxation times are Auger dominated.<sup>10</sup> Recent experimental studies of the ground and excited state recovery as a function of the injection current have also suggested that the ultrafast relaxation processes are Auger dominated.<sup>8</sup>

Here, we present an analysis of the intermediate recovery time scale which corresponds to the dot capture time, as a function of the injection current using time-resolved spec-

troscopy. By focusing on the dependence of the dot capture time on bias level and performing theoretical calculations to interpret our results, we highlight the importance of Auger effects in this slower component of the gain recovery. It is worthwhile pointing out that the carrier dynamics at this time scale currently constitutes the main limitation for high speed optical information processing applications when the device is operated in the ground state saturated regime (i.e., maximally inverted), and thus it is vital that the underlying physical mechanisms for this process be well understood.

The experimental arrangement is very similar to that presented originally in Ref. 5. Pulses of about 300 fs pulse width at 1.32  $\mu\text{m}$  were obtained from a titanium-sapphire pumped, optical parametric oscillator (OPO). The pump-probe differential transmission was measured using a heterodyne detection as in Ref. 5. Briefly, the output of the OPO was split into three beams (reference, pump, and probe). Acousto-optic modulators were used to shift the frequency of the probe and reference beams by 80 and 79 MHz, respectively. After propagation through the amplifier with suitable delays, the probe and reference beams were overlapped on a slow detector. The amplitude of the difference frequency (1 MHz) was detected using a high frequency lock-in amplifier. This signal is proportional to the transmission of the amplifier. The QD SOAs were 3 mm long, 4  $\mu\text{m}$  width ridges with tilted, antireflection coated facets, and were fabricated from material which consisted of six stacks of InAs/GaAs QDs in a dots-in-a-well structure, grown by Zia Inc. and operating at 1.32  $\mu\text{m}$  (for further details see Ref. 11). Figure 1 shows the characteristic amplified spontaneous emission as a function of bias level, showing the appearance of the ground and excited states at 1320 and 1250 nm, respectively. An example of the gain recovery curve in the 0–8 ps range at a bias of 30 mA is shown on Fig. 2 and demonstrates the biexponential nature of the underlying processes for this range. For the remainder of this letter we will focus on the behavior of the longer of these two times (dot capture time) and thus we do not need to correct for nonlinearities and coherent artifacts that usually occur for very small pump-probe delays. A method for treating such nonlinearities is outlined in Ref. 12. Figure 3 shows the behavior of the capture time as a function of SOA bias current, plotted on a log-log scale, and demonstrating the power law behavior. From this graph, it is clear that there is a  $J^x$  dependence, where the exponent  $x$  was measured to be  $-0.6 \pm 0.1$ . The

<sup>a)</sup>Also at Cork Institute of Technology, Cork, Ireland; electronic mail: tomasz.piwonski@tyndall.ie

<sup>b)</sup>Also at Waterford Institute of Technology, Waterford, Ireland; electronic mail: johoul@gmail.com

<sup>c)</sup>Also at Cork Institute of Technology, Cork, Ireland.

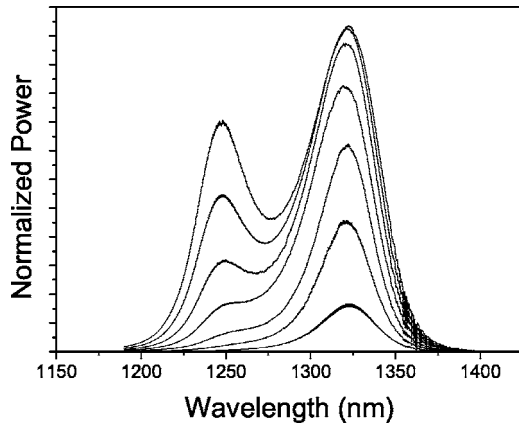


FIG. 1. Amplified spontaneous emission as a function of bias level for the QD device. The currents were 25, 50, 100, 125, 150, and 175 mA.

uncertainty in the slope is obtained statistically by performing many different scans, some with varying parameters such as pump and probe energies.

To understand the physics that leads to the observed power law behavior, we consider a rate equation model of quantum dot carrier dynamics, similar to Ref. 13. The system is described in terms of separate normalized carrier density states (wetting layer  $N_{wl}$  pumped by  $J$ , excited state  $N_e$ , ground state  $N_g$ ) with capture and escape terms between adjacent states and interband recombination for each state. The key feature of the model is that the physics of the capture/escape and recombination processes can be expressed through the parameters  $\alpha$  and  $\beta$ , respectively. For the capture/escape terms,  $\alpha=1$  corresponds to a phonon assisted capture/escape, while  $\alpha=2$  or higher corresponds to Auger-type capture/escape processes. The recombination terms are parametrized by  $\beta$ , with  $\beta=1$  describing a monomolecular process,  $\beta=2$  describing spontaneous emission, and  $\beta=3$  describing an Auger dominated process. The equations read

$$\dot{N}_{wl} = J - \gamma_1 N_{wl}^\alpha (1 - N_e) + \epsilon_1 \gamma_1 N_e^\alpha - \gamma_3 N_{wl}^\beta,$$

$$\begin{aligned} \dot{N}_e = & \gamma_1 N_{wl}^\alpha (1 - N_e) - \epsilon_1 \gamma_1 N_e^\alpha - \gamma_2 N_e^\alpha (1 - N_g) \\ & + \epsilon_2 \gamma_2 N_g^\alpha (1 - N_e) - \gamma_4 N_e^\beta, \end{aligned}$$

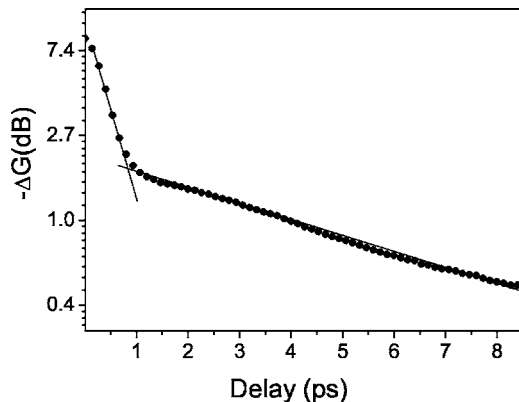


FIG. 2. Pump induced gain change as a function of pump-probe delay showing the biexponential behavior. The amplifier bias was 30 mA.

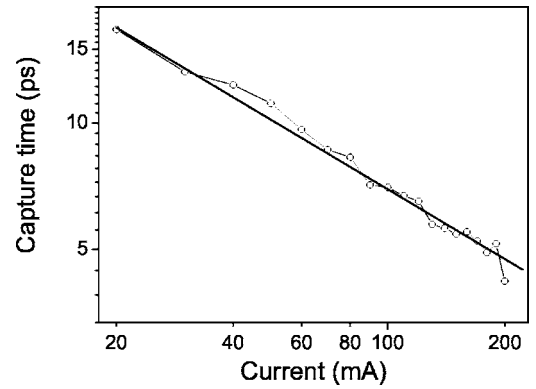


FIG. 3. Plot of dot capture time as a function of bias current showing the power law behavior. The fitted exponent is  $-0.6 \pm 0.1$ .

$$\dot{N}_g = \gamma_2 N_e^\alpha (1 - N_g) - \epsilon_2 \gamma_2 N_g^\alpha (1 - N_e) - \gamma_5 N_g^\beta. \quad (1)$$

The parameters  $\gamma_1$  and  $\gamma_2$  determine the strength of the capture processes into the excited and ground states, respectively, while  $\epsilon_1$  and  $\epsilon_2$  do similarly for the escape processes from these states. The  $(1-N)$  terms are Pauli blocking factors for ground and excited states. The  $\gamma_4$ ,  $\gamma_5$ , and  $\gamma_6$  parameters scale the strength of the wetting layer, excited state, and ground state recombination processes, respectively, and were set to one for the remainder of this letter.

A numerical stability analysis of this system of equations was performed in order to calculate the capture time of the excited state from the wetting layer as a function of bias level (shown on Fig. 4 for  $\alpha=2$  and  $\beta=3$ , other parameters in caption). The capture time (solid line) displays a power law behavior for high pump levels; the corresponding exponent of  $-0.69$  over the fitted region (dots) is in general agreement with the experimental results. These values for  $\alpha$  and  $\beta$  correspond to Auger processes for both the capture and recombination times. Since previous studies have shown that Auger effects dominate the interband relaxation processes,<sup>10</sup> we can conclude that Auger mediated carrier capture is necessary to reproduce the experimentally observed behavior.

Equations (1) can be further simplified, under the assumptions that the scattering between excited and ground states is much faster than the excited state capture from the wetting layer and the excited state evaporation is negligible. In this case, the equations can be simplified to read

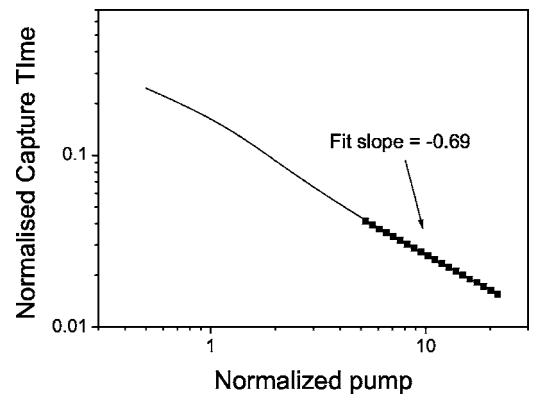


FIG. 4. Plot of calculated dot capture time using Eq. (1) as a function of bias current (thin line). Note that for high pump, the graph displays a power law behavior with a fitted exponent of  $-0.69$ . The parameters of the model were  $\gamma_1=10$ ,  $\gamma_2=1000$ ,  $\epsilon_1=0.005$ , and  $\epsilon_2=0.2$ .

TABLE I. Dot capture time as a function of  $\alpha$  for Eq. (1) using a linear stability analysis technique.

| $\alpha=1$                          | $\alpha=2$                          |
|-------------------------------------|-------------------------------------|
| $\tau_2 \sim 1/\gamma_1(J-1)^{1/3}$ | $\tau_2 \sim 1/\gamma_1(J-1)^{2/3}$ |

$$\begin{aligned} \dot{N}_{wl} &= J - \gamma_1 N_{wl}^\alpha (1 - N_g) - N_{wl}^\beta, \\ \dot{N}_g &= \gamma_1 N_{wl}^\alpha (1 - N_g) - N_g^\beta. \end{aligned} \quad (2)$$

For high pump levels, it is possible to obtain an analytical expression for the carrier relaxation time into the dot. Again, we assume that Auger effects are the main interband relaxation processes in accordance with Ref. 10 and set  $\beta=3$ . Table I summarizes the expressions for both the phonon assisted ( $\alpha=1$ ) and Auger ( $\alpha=2$ ) cases. It is evident that  $\alpha=2$  is required to reproduce the experimental behavior, resulting in a  $J^{-2/3}$  trend. Thus, an Auger capture process results in good agreement with our experimental results.

In conclusion, we have used a heterodyne pump-probe method to determine the dependence of the capture time of InAs/GaAs quantum dots on bias current. The measured power law relationship between these two quantities was in good agreement with a model which assumed Auger dominated capture and recombination processes. This finding is important for future optical information processing applications since it implies that the recovery time of the ground state gain should be extremely fast for sufficiently high current levels.

The authors would like to acknowledge Christopher Roche and John Lucy for technical assistance. This study has

been supported by Science Foundation Ireland (SFI) under Contract Nos. 01/FI/CO13 and 03/IN.1/1340, the Irish Research Council for Science, Engineering and Technology (IRCSET), through the Tyndall National Access Programme, and the Irish Higher Education Authority under the PRTL program.

- <sup>1</sup>D. Bimberg, M. Grundmann, and N. N. Ledentsov, *Quantum Dot Heterostructures* (Wiley, New York, 1999).
- <sup>2</sup>D. O'Brien, S. P. Hegarty, G. Huyet, J. G. McInerney, T. Kettler, M. Laemmlin, D. Bimberg, V. M. Ustinov, A. E. Zhukov, S. S. Mikhlin, and A. R. Kovsh, *Electron. Lett.* **39**, 1819 (2003).
- <sup>3</sup>T. Akiyama, N. Hatori, Y. Nakata, H. Ebe, and M. Sugawara, *Electron. Lett.* **38**, 1139 (2002).
- <sup>4</sup>A. V. Uskov, E. P. O'Reilly, R. J. Manning, R. P. Webb, D. Cotter, M. Laemmlin, N. N. Ledentsov, and D. Bimberg, *IEEE Photonics Technol. Lett.* **16**, 1265 (2004).
- <sup>5</sup>K. L. Hall, G. Lenz, E. P. Ippen, and G. Raybon, *Opt. Lett.* **17**, 874 (1992).
- <sup>6</sup>P. Borri, W. Langbein, J. M. Hvam, F. Heinrichsdorff, M.-H. Mao, and D. Bimberg, *IEEE Photonics Technol. Lett.* **12**, 6 (2000).
- <sup>7</sup>P. Borri, S. Schneider, W. Langbein, U. Woggon, A. E. Zhukov, V. M. Ustinov, N. N. Ledentsov, Zh. I. Alferov, D. Ouyang, and D. Bimberg, *Appl. Phys. Lett.* **79**, 2633 (2001).
- <sup>8</sup>S. Schneider, P. Borri, W. Langbein, U. Woggon, R. L. Sellin, D. Ouyang, and D. Bimberg, *IEEE Photonics Technol. Lett.* **17**, 10 (2005).
- <sup>9</sup>M. van der Poel, J. Mrk, A. Somers, A. Forchel, J. P. Reithmaier, and G. Eisenstein, *Appl. Phys. Lett.* **89**, 081102 (2006).
- <sup>10</sup>I. P. Marko, A. D. Andreev, A. R. Adams, R. Krebs, J. P. Reithmaier, and A. Forchel, *Electron. Lett.* **39**, 1 (2003).
- <sup>11</sup>T. C. Newell, D. J. Bossert, A. Stintz, B. Fuchs, K. J. Malloy, and L. F. Lester, *IEEE Photonics Technol. Lett.* **11**, 12 (1999).
- <sup>12</sup>P. Borri, F. Romstad, W. Langbein, A. Kelly, J. Mork, and J. Hvam, *Opt. Express* **7**, 107 (2000).
- <sup>13</sup>T. W. Berg, S. Bischoff, I. Magnusdottir, and J. Mork, *IEEE Photonics Technol. Lett.* **13**, 6 (2001).